



Luttinger Liquid of Polarons in One-Dimensional Boson-Fermion Mixtures

Citation

Mathey, L., D.-W. Wang, W. Hofstetter, M. D. Lukin, and Eugene Demler. 2004. "Luttinger Liquid of Polarons in One-Dimensional Boson-Fermion Mixtures." *Physical Review Letters* 93 (12) (September 14). doi:10.1103/physrevlett.93.120404. <http://dx.doi.org/10.1103/PhysRevLett.93.120404>.

Published Version

doi:10.1103/PhysRevLett.93.120404

Permanent link

<http://nrs.harvard.edu/urn-3:HUL.InstRepos:27899429>

Terms of Use

This article was downloaded from Harvard University's DASH repository, and is made available under the terms and conditions applicable to Other Posted Material, as set forth at <http://nrs.harvard.edu/urn-3:HUL.InstRepos:dash.current.terms-of-use#LAA>

Share Your Story

The Harvard community has made this article openly available. Please share how this access benefits you. [Submit a story](#).

[Accessibility](#)

Luttinger Liquid of Polarons in One-Dimensional Boson-Fermion Mixtures

L. Mathey, D.-W. Wang, W. Hofstetter, M. D. Lukin, and Eugene Demler

Physics Department, Harvard University, Cambridge, Massachusetts 02138, USA

(Received 22 January 2004; published 14 September 2004)

We use the bosonization approach to investigate quantum phases of boson-fermion mixtures (BFM) of atoms confined to one dimension by an anisotropic optical lattice. For a BFM with a single species of fermions we find a charge-density wave phase, a fermion pairing phase, and a phase separation regime. We also obtain the rich phase diagram of a BFM with two species of fermions. We demonstrate that these phase diagrams can be understood in terms of polarons, i.e., atoms “dressed” by screening clouds of the other atom species. Techniques to detect the resulting quantum phases are discussed.

DOI: 10.1103/PhysRevLett.93.120404

PACS numbers: 03.75.Mn, 71.10.Pm, 71.38.-k

Mixtures of ultracold bosonic and fermionic atoms, which have recently become accessible experimentally, represent a promising new system for studying strongly correlated many-body physics [1]. In addition, by loading atoms in anisotropic lattices, several recent experiments produced 1D systems of ultracold atoms [2]. Several novel phenomena have been predicted theoretically for boson-fermion mixtures (BFM) including pairing of fermions [3], formation of composite particles [4], and spontaneous breaking of translational symmetry in optical lattices [5]. Most of these theoretical studies relied on a mean-field approach to investigate many-body states of fermions. This approach, however, becomes unreliable in the regime of strong interactions. In particular, it fails in low-dimensional systems due to enhanced fluctuations and nonperturbative effects of interactions.

In this Letter we use the bosonization method [6,7] to investigate one-dimensional (1D) BFM. The resulting quantum phases can be understood by introducing polarons, i.e., atoms of one species surrounded by screening clouds of the other species. In our analysis the polarons emerge as the most well-defined quasiparticles in the interacting system, while quantum phases of the system arise from a competition of various ordering instabilities of such polarons. The phase diagrams we obtain show a remarkable similarity to the Luttinger liquid (LL) phase diagrams of 1D interacting electron systems [8], suggesting that 1D BFM may be understood as LLs of polarons.

In Fig. 1 we show a typical phase diagram for a BFM as a function of experimentally controlled parameters: the scattering length between bosons and fermions (a_{bf}) and the strength of the longitudinal optical lattice for bosonic atoms ($V_{b,\parallel}$) [9]. For relatively weak interactions and slow bosons (i.e., large $V_{b,\parallel}$) the system is in the charge-density-wave (CDW) phase, in which the densities of fermions and bosons have a periodic modulation [10]. For very strong interactions the system is unstable to phase separation (PS) [11,12]. The two regimes are separated by a p -wave pairing phase of fermionic polarons (f -PP). Our analysis is carried out for the most promising system of

atoms in an optical lattice. However, qualitative results should also apply to atoms in a tight 1D cigar-shaped magnetic trap [13].

The essence of the bosonization procedure is to diagonalize the effective low-energy Hamiltonian, which allows for the exact calculation of all relevant correlation functions. The phase diagrams are determined by finding the order parameter which has the most divergent susceptibility [8]. Bosonization approach has been applied to BFM in Ref. [11]. This work pointed out some of the gapped phases but did not consider correlations of polaronic degrees of freedom. Including the latter leads to a much richer phase diagram which we discuss below. The present system also has a close analogy to 1D electron-phonon systems discussed previously (see, e.g., Ref. [14]). A qualitative difference of the electron-phonon system is

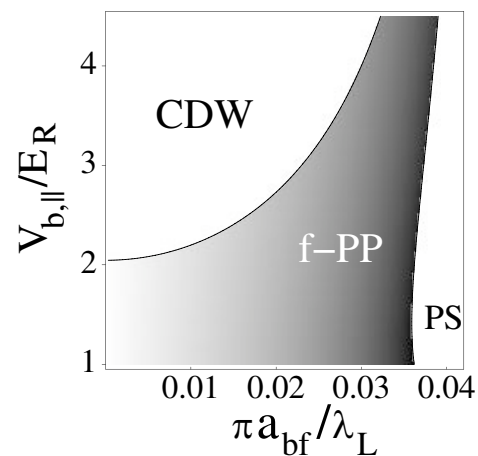


FIG. 1. Phase diagram for a mixture of bosonic and spinless fermionic atoms. Shading in the f -PP phase describes the strength of the bosonic screening cloud [2a; see Eq. (4)] around a pair of fermions. λ_L and E_R are, respectively, the lattice period and recoil energy. Other parameters used for this figure are (see the text for notations) $\nu_b = 4$, $\nu_f = 0.5$, $V_{b,\perp} = V_{f,\perp} = 20E_R$, $V_{f,\parallel} = 2E_R$, and boson-boson scattering length $a_{bb} = 0.01\lambda_L$.

that the sound velocity is usually much smaller than the Fermi velocity, whereas for a BFM the velocity of the phonon modes (of the bosonic condensate) can be larger than the Fermi velocity. We also note that the 1D p -wave superfluid we obtain here may be of relevance to a recent proposal for quantum computation [15].

We first consider a mixture of spinless fermionic (f) and bosonic (b) atoms. For sufficiently strong optical potential the microscopic Hamiltonian is given by a single band Hubbard model

$$H = -\sum_{\langle ij \rangle} (t_b b_i^\dagger b_j + t_f f_i^\dagger f_j) - \sum_i (\mu_f n_{f,i} + \mu_b n_{b,i}) + \frac{U_b}{2} \sum_i n_{b,i} (n_{b,i} - 1) + U_{bf} \sum_i n_{b,i} n_{f,i}, \quad (1)$$

where $n_{b/f,i}$ are the boson/fermion density operators with $\mu_{b/f}$ being their chemical potentials. The tunneling amplitudes $t_{f/b}$ and the particle interactions U_b and U_{bf} can be expressed explicitly in terms of the s -wave scattering lengths, the laser beam intensities, and the atomic masses [16]. For simplicity we assume that the filling fraction of fermions $\nu_f \equiv \langle n_{f,i} \rangle$ is not commensurate with the lattice or with the filling fraction of bosons ν_b . The Fermi momentum and velocity are given by $k_f = \pi \nu_f$ and $v_f = 2t_f \sin(k_f)$, respectively.

In Haldane's bosonization approach [6,7] 1D fermion and boson operators can be represented by $f(x) = [\nu_f + \Pi_f]^{1/2} \sum_{m=-\infty}^{\infty} e^{(2m+1)i\Theta_f} e^{i\Phi_f}$ and $b(x) = [\nu_b + \Pi_b]^{1/2} \times \sum_{m=-\infty}^{\infty} e^{2mi\Theta_b} e^{i\Phi_b}$, where x is a continuous coordinate that replaces the site index i . The operators $\Pi_{f/b}(x)$ and $\Phi_{f/b}(x)$ are, respectively, the bosonized density and phase fluctuation operators. The $\Theta_{f/b}(x)$ fields are given by $\Theta_{f/b} \equiv \pi \nu_{f/b} x + \pi \int^x dy \Pi_{f/b}(y)$. The low-energy effective Hamiltonian thus can be written as

$$H_{\text{eff}} = \sum_{\alpha=b,f} \frac{v_\alpha}{2} \int dx \left[\frac{K_\alpha}{\pi} (\partial_x \Phi_\alpha)^2 + \frac{\pi}{K_\alpha} \Pi_\alpha^2 \right] + U_{bf} \int dx \Pi_b \Pi_f + \frac{2G}{2\pi} \int dx [\pi^2 \Pi_f^2 - (\partial_x \Phi_f)^2], \quad (2)$$

where v_b and K_b are the phonon velocity and Luttinger exponent of the bosons and $K_f = 1$ for noninteracting fermion atoms. To obtain the last term of H_{eff} we have integrated out the high energy ($2k_f$) phonons within the instantaneous approximation (i.e., assuming $v_b \gg v_f$). $G \equiv g_{2k_f}^2 / \omega_{2k_f}$, where ω_k is the (Bogoliubov) phonon energy dispersion [17] and $g_k = U_{bf} \sqrt{v_b \varepsilon_{b,k} / 2\pi \omega_k}$ is the fermion-phonon (FP) coupling vertex with $\varepsilon_{b,k}$ being the noninteracting boson band energy. In the long wavelength limit we have a conventional FP coupling $g_k = g|k|^{1/2}$ with $g \equiv U_{bf} \sqrt{K_b} / 2\pi$. The effective Hamiltonian, Eq. (2), is quadratic and can be diagonalized [18]. The resulting two eigenmode velocities are

given by [11]

$$v_{a,A}^2 = \frac{1}{2}(v_b^2 + \tilde{v}_f^2) \pm \frac{1}{2} \sqrt{(v_b^2 - \tilde{v}_f^2)^2 + 16\tilde{g}^2 v_b \tilde{v}_f}, \quad (3)$$

where $\tilde{v}_f \equiv (v_f^2 - 4G^2)^{1/2}$ and $\tilde{g} \equiv g e^\theta$ with $e^\theta = [(v_f - 2G)/(v_f + 2G)]^{1/4}$. When the FP coupling g becomes sufficiently strong the eigenmode velocity v_A becomes imaginary, indicating an instability of the system. This instability corresponds to phase separation (global collapse) for positive (negative) U_{bf} [11].

To understand the nature of the many-body state of BFM outside of the instability region we analyze the long-distance behavior of the correlation functions. For the bare bosonic and fermionic particles we find $\langle b(x)b^\dagger(0) \rangle \sim |x|^{-\frac{1}{2}K_\epsilon^{-1}}$ and $\langle f(x)f^\dagger(0) \rangle \sim \cos(k_f x) |x|^{-\frac{1}{2}(K_\beta + K_\gamma^{-1})}$ [19]. To describe particles dressed by the other species we introduce the composite operators

$$\tilde{f}(x) \equiv e^{-i\lambda\Phi_b(x)} f(x), \quad \tilde{b}(x) \equiv e^{-i\eta\Phi_f(x)} b(x), \quad (4)$$

with λ and η being some real numbers. The correlation functions of these operators are given by $\langle \tilde{f}(x)\tilde{f}^\dagger(0) \rangle \sim \cos(k_f x) |x|^{-\frac{1}{2}(K_\beta + \lambda^2 K_\epsilon^{-1} + K_\gamma^{-1} - 2\lambda K_\gamma^{-1})}$ and $\langle \tilde{b}(x)\tilde{b}^\dagger(0) \rangle \sim |x|^{-\frac{1}{2}(K_\epsilon^{-1} + \eta^2 K_\gamma^{-1} - 2\eta K_\gamma^{-1})}$ [19]. We observe that the exponents of the correlation functions are maximized for $\lambda_c = K_\epsilon / K_\gamma \epsilon$ and $\eta_c = K_\gamma / K_\gamma \epsilon$. From now on we use Eq. (4) with λ_c and η_c to construct polaronic particles. In the limit of weak interactions we have $\lambda_c \rightarrow U_{bf}/U_b$ and $\eta_c \rightarrow 2U_{bf}/\pi v_b$. This result can be understood by a simple density counting argument that a fermionic polaron (f -polaron) locally suppresses (enhances) a bosonic cloud by λ_c particles, whereas a bosonic polaron (b -polaron) depletes (enhances) the fermionic system by η_c atoms for positive (negative) g .

The polaronic operators defined in Eq. (4) can also be introduced via the canonical polaron transformation (CPT) [20]. The CPT operator is given by $U = e^{-i\lambda \sum_{k \neq 0} (F_k \beta_k \rho_k^\dagger + \text{H.c.})}$, where β_k is the phonon annihilation operator, ρ_k is the fermion density operator, F_k is some function of wave vector k , and λ specifies the strength of the phonon dressing. When applied to a fermion operator, the CPT transforms it to a polaron operator, $U^{-1} f(x) U = f(x) \exp[-i\lambda \sum_{k \neq 0} (F_k \beta_k e^{-ik \cdot x} + \text{H.c.})]$ [20], which is the same as Eq. (4), provided that one takes $F_k = \sqrt{\frac{2\pi}{K_b |k| L}} \text{sgn}(k)$. (Note that in 1D fermionic systems density operators correspond to Luttinger bosons.) We note, however, unlike in ordinary polaron theory, where further approximations after the CPT have to be made [20], in the 1D BFM system we consider here, the full low-energy quantum fluctuations have been included via the bosonization method and exact diagonalization of the resulting Hamiltonian Eq. (2). This allows for an essentially exact determination of the polarization parameter λ .

Now we study the many-body ground state phase diagram of a 1D BFM, which is characterized by specifying the order parameters that have the slowest long-distance decay of the correlation functions [8]. Two types of ordering were found to occur: $2k_f$ ordering due to a Peierls-type instability and f -polaron pairing due to their effective attractive interactions induced by the screening clouds. For the $2k_f$ -CDW order parameter, $O_{\text{CDW}} = f_L^\dagger f_R$, we find $\alpha_{\text{CDW}} = 2 - 2K_\beta$, and for the f -PP field, $O_{f\text{-PP}} = \tilde{f}_L \tilde{f}_R$, we obtain $\alpha_{f\text{-PP}} = 2 - 2[\lambda_c^2 K_\epsilon^{-1} + K_\gamma^{-1} - 2\lambda_c K_\gamma^{-1}]$. We did not include polaron dressing in O_{CDW} , since this operator has no net fermionic charge and the exponent of O_{CDW} does not change if we replace f by \tilde{f} . Scaling exponents shown in Fig. 2(a) demonstrate that divergencies of the CDW and f -PP susceptibilities (corresponding to positive α) are mutually exclusive and cover the entire phase diagram outside the PS regime. In the same figure, we also show the scaling exponents calculated for bare fermion pairing ($O_{\text{BFP}} = f_L f_R$), bare boson condensate ($O_{\text{BB}} = b$), and b -polaron condensate ($O_{b\text{-P}} = \tilde{b}$). It is easy to see that the polaronic order parameters always have larger exponents than their counterparts constructed with bare atoms, showing the stability of a polaronic quasiparticle in a 1D BFM system. Moreover, the necessity to consider f -polaron pairing instead of bare fermion pairing is further supported by considering the stability of superfluidity: we introduce a single weak impurity potential in the 1D BFM and determine its relevance by a renormalization group (RG) calculation [21]. We find that the impurity potential is relevant within the CDW phase and irrelevant outside of it. This indicates that there should be a superfluid phase outside of the insulating CDW phase, which supports the existence of f -polaron pairing instead of bare fermion pairing according to Fig. 2(a).

In Fig. 2(b) we show a global phase diagram of a BFM considering the FP coupling (g) and effective fermion-fermion interaction (G) as independent variables. One can see that the polaronic effects and the associated pairing

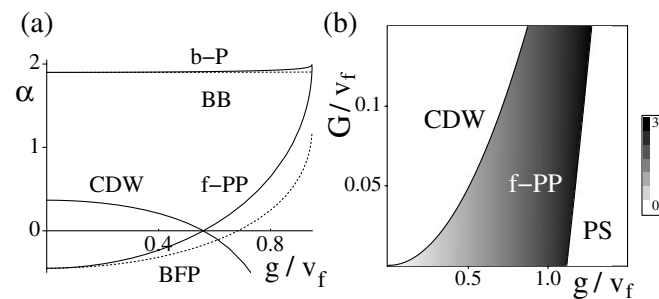


FIG. 2. Ground state of a BFM with spinless fermions. (a) Scaling exponents of different order parameters (see the text). Parameters are chosen to be $v_b/v_f = 3$, $K_b = 5$, and $G/v_f = 0.1$. (b) Global phase diagram for $v_b/v_f = 5$ and $K_b = 10$.

phase are important when FP coupling (g) is large, while the CDW phase dominates when the effective fermion interaction (G) is increased. This phase diagram is very similar to what one finds for spinless electrons in LL theory [8], where CDW and the pairing phase compete with each other in the whole phase diagram. Therefore one can introduce a LL of polarons to describe BFM in 1D. The phase diagram in terms of experimentally controlled parameters was shown in Fig. 1. When considering finite temperature effects in a realistic experiment, we note that the correlation function is cut off by thermal correlation lengths, which are approximately given by $\xi \sim v_f/k_B T$. Therefore the zero temperature ground states should appear when $\xi > L$ with L being the system size. This corresponds to a temperature regime of 1% of the Fermi temperature for systems of approximately 100 sites in the longitudinal direction.

Several approaches can be used to detect the quantum phases discussed above. First, in the CDW phase the fermion density modulation induces a $2k_f$ density wave in the boson field in addition to the zero momentum condensation so that the CDW phase can be observed as interference peaks at momentum $k = 2k_f$ in a standard time-of-flight (TOF) measurement for bosons [10]. Second, the polaron pairing phase can be observed by measuring the noise correlation of fermions in a TOF experiment as proposed in Ref. [22]. Third, a laser stirring experiment [23] can be used to probe the phase transition between the insulating (pinned by trap potential) CDW and the superfluid f -PP phase: one can use a laser beam focused at the center of the cloud and stir such local potential to measure the response of the BFM. If the system is in the pairing phase, the laser beam can be moved through the system without dissipation if only its velocity is slower than some critical value [23]. At the f -PP/CDW phase boundary this critical velocity goes to zero, reflecting a transition to the insulating (CDW) state. This scenario follows from the above described RG analysis of a single impurity potential [21]. Finally a way to probe the PS boundary could be to measure the dipolar collective oscillations of the system, generated by a sudden displacement of the harmonic trap potential with respect to the lattice potential [24]. When the system is near the PS boundary, the fermion-boson interaction strongly reduces the frequency of the dipolar mode.

The above analysis can be similarly applied to a BFM with fermions of two internal hyperfine states, which we assume to be SU(2) symmetric. Spin symmetry of the system leads to a separation of the bosonized Hamiltonian into spin and charge sectors. The charge part of the Hamiltonian is equivalent to a BFM with spinless atoms and can be diagonalized analogously. The spin part of the Hamiltonian has the standard form of a sine-Gordon model (SGM), $H_\sigma = \frac{1}{2} v_\sigma \int dx [\pi \Pi_\sigma^2 + \frac{1}{\pi} (\partial_x \Phi_\sigma)^2] + \frac{2g_{1\perp}}{(2\pi\alpha)^2} \int dx \cos[\sqrt{8K_\sigma} \Theta_\sigma]$, where v_σ is the spin velocity, K_σ is the spin Luttinger exponent, and

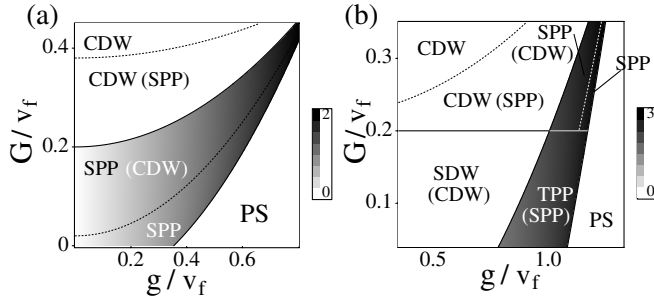


FIG. 3. Phase diagrams for a mixture of bosonic and $S = 1/2$ fermionic atoms with $v_b/v_f = 5$ and $K_b = 10$. In (a) $U_{\parallel}/v_f = -0.8\pi$ and in (b) $U_{\parallel}/v_f = 0.8\pi$. Note that parentheses (\cdots) indicate subdominant phases.

$g_{1\perp} = U_{\parallel} - 4\pi G$ is the effective backward scattering amplitude for fermions, which has contributions from the bare fermion-fermion interaction and from integrating out $2k_f$ phonons. The nature of spin excitations in the ground state follows from the well-known properties of the SGM: For $K_{\sigma} > 1$ the system has gapless spin wave excitations ($g_{1\perp}$ is irrelevant) and for $K_{\sigma} < 1$ the system has a spin gap ($g_{1\perp}$ becomes relevant) [25]. In Fig. 3 we show the quantum phase diagram of a BFM with $S = 1/2$ fermions. Because of the larger number of degrees of freedom more types of ordering are possible: in addition to the CDW phase, we have a spin density wave (SDW), where the spin order parameter at wave vector $2k_f$ ($O_{\text{SDW}} = \sum_{s,s'} f_{s,L}^{\dagger} \hat{\sigma}_{s,s'} f_{s',R}$ with $\hat{\sigma}_{\alpha\beta}$ being the Pauli matrix) develops quasi-long-range order. For the polaron pairing phase, both singlet (SPP, $O_{\text{SPP}} = \tilde{f}_{\downarrow,L} \tilde{f}_{\downarrow,R} - \tilde{f}_{\uparrow,L} \tilde{f}_{\uparrow,R}$) and triplet (TPP, $O_{\text{TPP}} = \tilde{f}_{\downarrow,L} \tilde{f}_{\uparrow,R}$) pairing can be realized in different regimes. Some of these quantum phases can coexist in certain regimes of the phase diagram (see Fig. 3). The remarkable feature of these diagrams is again its similarity to the phase diagram of 1D interacting electron (LL) systems [8]. These phases can also be detected by the experimental method suggested above for a BFM of spinless fermions. Note that in the regime where CDW or SPP phases dominate, a true long-distance order and finite spin gap are established due to the relevance of the backward scattering, $g_{1,\perp}$, which is negative in this regime. Such a gapped pairing phase is actually the molecule liquid in a 1D system and therefore should be experimentally observable by the recently developed techniques of rf photodissociation [26].

In summary, we used the bosonization method to investigate the quantum phases of 1D BFM involving spinless and $S = 1/2$ fermions. The rich phase diagrams that we found can be understood in terms of a LL of polarons. We also described several experimental techniques for probing these quantum phases.

We thank B. I. Halperin for valuable discussions. This work was supported by the NSF (Grants No. DMR-01328074 and No. PHY-0134776), by the Sloan and the

Packard Foundations, and by Harvard-MIT CUA. W. H. was supported by the German Science Foundation (DFG).

- [1] G. Modugno *et al.*, *Science* **297**, 2240 (2002); F. Ferlaino *et al.*, *Phys. Rev. Lett.* **92**, 140405 (2004).
- [2] B. Laburthe Tolra *et al.*, *Phys. Rev. Lett.* **92**, 190401 (2004); T. Stöferle *et al.*, *Phys. Rev. Lett.* **92**, 130403 (2004).
- [3] F. Matera, *Phys. Rev. A* **68**, 043624 (2003); D. V. Efremov and L. Viverit, *Phys. Rev. B* **65**, 134519 (2002); L. Viverit, *Phys. Rev. A* **66**, 023605 (2002).
- [4] M. Y. Kagan *et al.*, cond-mat/0209481.
- [5] R. Roth and K. Burnett, *Phys. Rev. A* **69**, 021601 (2004); H. P. Büchler and G. Blatter, *Phys. Rev. Lett.* **91**, 130404 (2003); T. Miyakawa *et al.*, cond-mat/0401107.
- [6] F. D. M. Haldane, *Phys. Rev. Lett.* **47**, 1840 (1981).
- [7] M. A. Cazalilla, *J. Phys. B* **37**, S1 (2004).
- [8] J. Solyom, *Adv. Phys.* **28**, 201 (1979); J. Voit, *Rep. Prog. Phys.* **58**, 977 (1995).
- [9] In this Letter, we use $V_{f/b,\parallel(\perp)}$ to denote the optical lattice potential experienced by fermionic/bosonic atoms in the longitudinal (perpendicular) directions.
- [10] We note that in a homogeneous 1D system only quasi-long-range order for the CDW phase is possible. However, the inhomogeneous trap boundary in a realistic experiment can pin the CDW phase to generate a true density modulation.
- [11] M. A. Cazalilla *et al.*, *Phys. Rev. Lett.* **91**, 150403 (2003).
- [12] A. P. Albus *et al.*, *Phys. Rev. A* **67**, 063606 (2003); M. J. Bijlsma *et al.*, *Phys. Rev. A* **61**, 053601 (2000).
- [13] A. Görlitz *et al.*, *Phys. Rev. Lett.* **87**, 130402 (2001).
- [14] J. Voit and H. J. Schulz, *Phys. Rev. B* **36**, 968 (1987); **37**, 10068 (1988).
- [15] A. Y. Kitaev, cond-mat/0010440.
- [16] D. Jaksch *et al.*, *Phys. Rev. Lett.* **81**, 3108 (1998).
- [17] S. Tsuchiya and A. Griffin, cond-mat/0311321.
- [18] S. Engelsberg *et al.*, *Phys. Rev.* **136**, A1582 (1964).
- [19] Here we defined $K_{\beta} \equiv e^{2\theta} \tilde{v}_f (\cos^2 \psi / v_A + \sin^2 \psi / v_a)$, $K_{\delta} \equiv K_b v_b (\sin^2 \psi / v_A + \cos^2 \psi / v_a)$, $K_{\gamma}^{-1} \equiv e^{-2\theta} / \tilde{v}_f (v_A \cos^2 \psi + v_a \sin^2 \psi)$, $K_{\epsilon}^{-1} \equiv K_b^{-1} / v_b (v_A \sin^2 \psi + v_a \sin^2 \psi)$, $K_{\beta\delta} = e^{\theta} \sqrt{K_b \tilde{v}_f v_b} \sin(2\psi) / 2(1/v_a - 1/v_A)$, and $K_{\gamma\epsilon}^{-1} = e^{-\theta} / \sqrt{K_b \tilde{v}_f v_b} \sin(2\psi) / 2(v_a - v_A)$. ψ is given by $\tan 2\psi = 4\tilde{g}(v_b \tilde{v}_f)^{1/2} / (v_b^2 - \tilde{v}_f^2)$. These expressions are obtained from diagonalizing H_{eff} . Details will appear elsewhere.
- [20] G. D. Mahan, *Many-Particle Physics* (Plenum Press, New York, 1990); A. S. Alexandrov *et al.*, *Polarons and Bipolarons* (World Scientific, Singapore, 1995).
- [21] C. Kane *et al.*, *Phys. Rev. Lett.* **68**, 1220 (1992).
- [22] E. Altman *et al.*, cond-mat/0306226.
- [23] C. Raman *et al.*, *Phys. Rev. Lett.* **83**, 2502 (1999); R. Onofrio *et al.*, *Phys. Rev. Lett.* **85**, 2228 (1999).
- [24] P. Maddaloni *et al.*, *Phys. Rev. Lett.* **85**, 2413 (2000); S. D. Geneser and D. S. Jin, *Phys. Rev. Lett.* **87**, 173201 (2001); L. Vichi *et al.*, *Phys. Rev. A* **60**, 4734 (1999).
- [25] A. O. Gogolin, A. A. Nersisyan, and A. M. Tsvelik, *Bosonization and Strongly Correlated Systems* (Cambridge University Press, Cambridge, 1998).
- [26] C. A. Regal *et al.*, *Nature (London)* **424**, 47 (2003).